https://doi.org/10.4047/jap.2025.17.2.101

Effects of dental implant surface treated with sandblasting large grit acid-etching and femtosecond laser on implant stability, marginal bone volume, and histological results in a rabbit model

Young-Tak Son[1,a], KeunBaDa Son[2,a], Hoseong Cho[3,a], Jae-Mok Lee[4], Sm Abu Saleah[5], JunHo Hwang[6], JongHoon Lee[6], HyunDeok Kim[6], Myoung-Uk Jin[7], Jeehyun Kim[3], Mansik Jeon[3], Kyu-Bok Lee[2,8]*

[1]Department of Dental Science, Graduate School, Kyungpook National University, Daegu, Republic of Korea
[2]Advanced Dental Device Development Institute, Kyungpook National University, Daegu, Republic of Korea
[3]School of Electronic and Electrical Engineering, College of IT Engineering, Kyungpook National University, Daegu, Republic of Korea
[4]Department of Periodontology, School of Dentistry, Kyungpook National University, Daegu, Republic of Korea
[5]ICT Convergence Research Center, Kyungpook National University, Daegu, Republic of Korea
[6]Institute of Advanced Convergence Technology, Kyungpook National University, Daegu, Republic of Korea
[7]Department of Conservative Dentistry, School of Dentistry, Kyungpook National University, Daegu, Republic of Korea
[8]Department of Prosthodontics, School of Dentistry, Kyungpook National University, Daegu, Republic of Korea

ORCID
Young-Tak Son
https://orcid.org/0000-0001-8893-5369
KeunBaDa Son
https://orcid.org/0000-0002-3177-8005
Hoseong Cho
https://orcid.org/0000-0002-6091-1450
Jae-Mok Lee
https://orcid.org/0000-0002-0291-6114
Sm Abu Saleah
https://orcid.org/0000-0002-8129-4455
JunHo Hwang
https://orcid.org/0000-0002-3440-7218
JongHoon Lee
https://orcid.org/0000-0003-4184-3656
HyunDeok Kim
https://orcid.org/0000-0003-2921-8161
Myoung-Uk Jin
https://orcid.org/0000-0001-9263-047X
Jeehyun Kim
https://orcid.org/0000-0002-6170-0866
Mansik Jeon
https://orcid.org/0000-0002-0630-9039
Kyu-Bok Lee
https://orcid.org/0000-0002-1838-7229

Corresponding author
Kyu-Bok Lee
Department of Prosthodontics, School of Dentistry, Kyungpook National University, 2177 Dalgubuldaero, Jung-gu, Daegu, 41940, Republic of Korea
Tel +82 53 600 7674
E-mail kblee@knu.ac.kr

[a] These authors contributed equally to this work.

PURPOSE. The purpose of this study was to compare the surface characteristics and healing patterns after implantation of implants treated with SLA and those treated with both SLA and femtosecond laser. **MATERIALS AND METHODS.** A total of 10 male New Zealand white rabbits were used to compare recovery levels between implants treated with SLA (SLA group) and those treated with both SLA and femtosecond laser (SF group). The implants' surface characteristics were determined through topographic evaluation, element analysis, surface roughness, and wettability evaluation. In total, 4 implants were placed in each rabbit (2 in each tibia), with 20 implants per treatment group. Using the implant stability quotient (ISQ), marginal bone volume, and histological analysis (bone-to-implant contact (BIC), bone volume/tissue volume (BV/TV)), and post implantation outcomes were assessed. Outcome data were analyzed using independent t-tests, Mann-Whitney U tests, Wilcoxon signed-rank tests, and one-way ANOVA ($\alpha = 0.05$). **RESULTS.** No significant differences were noted between SLA and SF groups in terms of ISQ, marginal bone volume, BIC, and BV/TV ($P > .05$). However, significant differences in ISQ were observed within each group over time ($P < .05$). Furthermore, significant differences were noted in the marginal bone volume of the SF group ($P < .05$) and the BV/TV of the SLA group between weeks 4 and 6 ($P <$

Received November 5, 2024 / **Last Revision** March 10, 2025 / **Accepted** April 9, 2025

This work was supported by the NRF (No. 2022R1C1C2007040, MSIT) and KEIT (No. 20018114, MOTIE).

https://doi.org/10.4047/jap.2025.17.2.101

.05). **CONCLUSION.** Surface treatment via SLA and femtosecond laser is feasible compared with SLA treatment alone in terms of ISQ, marginal bone volume, BIC, and BV/TV. However, further clinical research is warranted. [J Adv Prosthodont 2025;17:101-14]

KEYWORDS
Dental implant surface treatment; Femtosecond laser; Implant stability; Osseointegration; Sandblasting acid-etching

INTRODUCTION

Dental implants, a popular method for replacing lost teeth, rely on osseointegration, which is the close contact between the bone and implant.[1,2] Surface design, which influences adhesion quality with osteoblasts, is a key parameter. Therefore, different surface treatment technologies such as sandblasting large grit acid-etching (SLA), laser application, and titanium plasma-spray have been developed.[3-5] Creating nano- and microscale physical topographies on implant surfaces positively influences biological osseointegration outcomes.[6,7] Increasing surface roughness to improve mechanical fixation between the bone and implant warrants further research.

The SLA method, commonly employed to commercial implants, involves blasting particles (250 – 500 μm) and chemically treating the surface with acid.[4,8] Although SLA improves osseointegration, it can lead to bacterial biofilm formation, potentially causing implant failure.[9-11] Thus, new technologies such as the femtosecond laser are being researched as alternatives for surface modification.[12,13] *In vitro* studies have demonstrated that femtosecond laser-treated implants decrease bacterial biofilm formation.[14,15] This laser technology can create complex structures on titanium surfaces with high precision, forming microscale physical topographies.[16,17] Despite its advantages, including enhanced osseointegration and reduced bacterial presence, research on bone integration with femtosecond laser-treated implants remains limited. Few studies have compared SLA and femtosecond laser-treated surfaces on discs *in vitro*. The current study aimed to observe and compare the outcomes of combining SLA and femtosecond laser treatment benefits in terms of osseointegration.

Previous research has quantitatively assessed surface roughness post-treatment using average surface roughness (Ra) and average absolute surface roughness (Sa) metrics.[18,19] Scanning electron microscope (SEM) evaluations, wettability evaluations, and topographical evaluations have been conducted.[20-22] Despite numerous studies, the optimal surface roughness and shape of implants remain undetermined. Continuous assessment is required for surfaces that exhibit appropriate roughness while inhibiting bacterial growth. Furthermore, evaluating the impact of these surfaces on actual osseointegration through *in vivo* studies following *in vitro* assessments is necessary.

In animal models, histological processing and morphological analysis are considered the gold standard for assessing dental implant osseointegration.[23-26] Implant stability quotient (ISQ) measurement and micro-computed tomography (CT) scans are also used to evaluate fixation and osseointegration.[27-29] However, micro-CT poses radiation risks and is typically conducted postmortem, making it challenging to compare pre- and post recovery bone states within the same subject.[30,31] Optical coherence tomography (OCT) could be an alternative, providing noninvasive, radiation-free features.[32-34] OCT allows immediate post implantation imaging and post sacrifice analysis, facilitating time-efficient and quantitative evaluations. However, no previous studies have used OCT to assess marginal bone volume after implantation. This study utilized OCT to image the surgical site immediately after implantation and post recovery, enabling evaluation of pre- and post recovery marginal bone volumes.

This study aimed to compare the surface characteristics (SEM, roughness, and wettability) of implants treated with SLA (SLA group) and those treated with both SLA and femtosecond laser (SF group) and to evaluate post-implantation healing in a rabbit model. Healing was assessed using ISQ, OCT for marginal bone volume, and histological analysis, including bone volume/tissue volume (BV/TV) ratio and bone-to-implant contact (BIC) ratio. The null hypothesis was that the surface treatment methods would not affect these parameters

MATERIALS AND METHODS

This study compared the extent of recovery in implants following surface treatment via SLA and SLA combined with femtosecond laser, as demonstrated in Figure 1. The implants were placed in the tibia of rabbits (10 subjects), and ISQ, OCT, and histological analyses were performed for osseointegration comparison.

Differences in the surface characteristics of implants treated with SLA and femtosecond laser were observed by creating implant discs for each surface type (Fig. 2). Five discs per surface type were ultrasonically cleaned for 15 min in a 1 : 1 : 1 (w/v/v) mixture of acetone, ethanol, and distilled water, then dried at 60°C for 2 h prior to observation. Surface images were captured using SEM (Hitachi SU8230; Hitachi, Tokyo, Japan) at an acceleration voltage 5 kV with 500× and 3500× magnifications for topographic evaluation. Using an energy dispersive X-ray spectroscopy (EDS) detector (Ultim Max 100; Oxford instruments, Abingdon, UK) (Fig. 2B), element analysis of the modified surfaces was performed. Surface roughness was quantitatively evaluated using confocal laser scanning microscopy (LEXT OLS4100; Olympus, Tokyo, Japan). Surface roughness was quantitatively assessed with

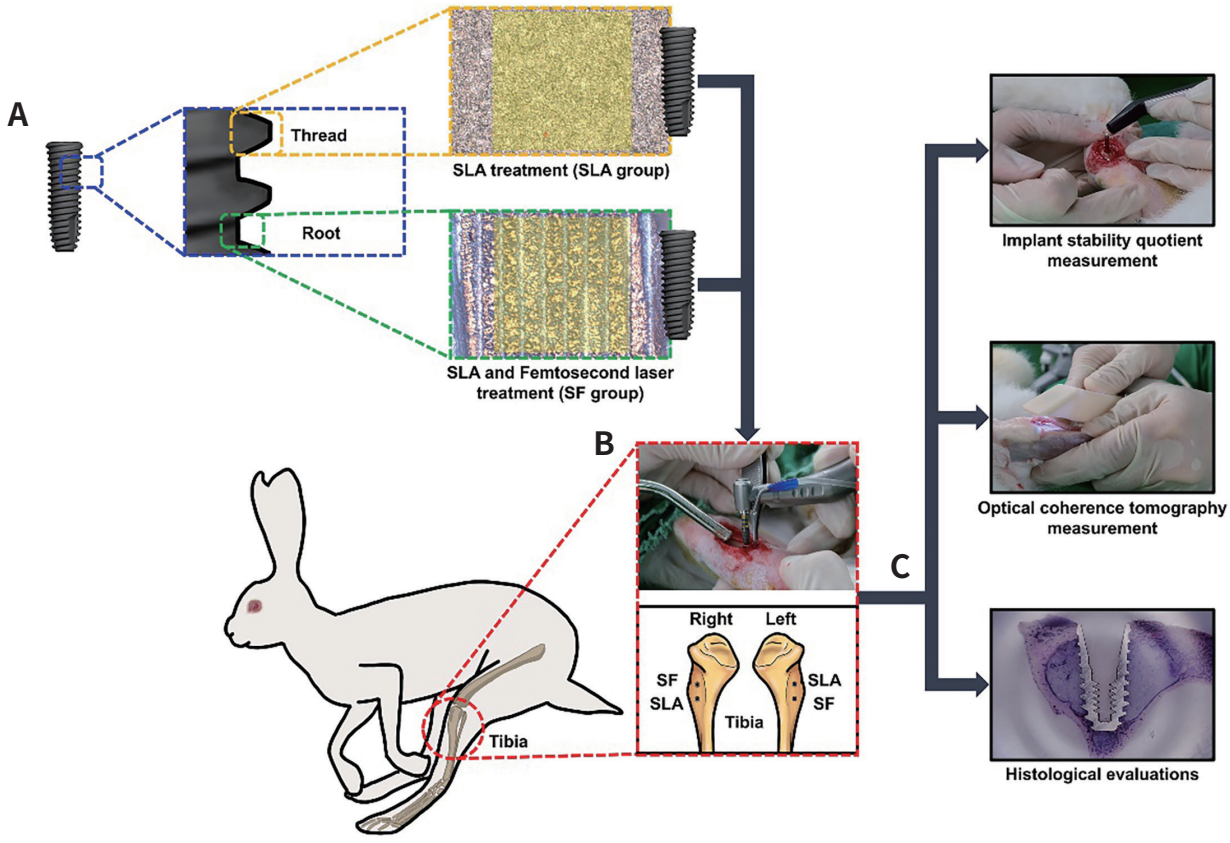

Fig. 1. Placement and evaluation process of each surface-treated implant. (A) Implant surface treatment method, (B) Placement process of each surface-treated implant, (C) Evaluation method after implant placement.

https://doi.org/10.4047/jap.2025.17.2.101

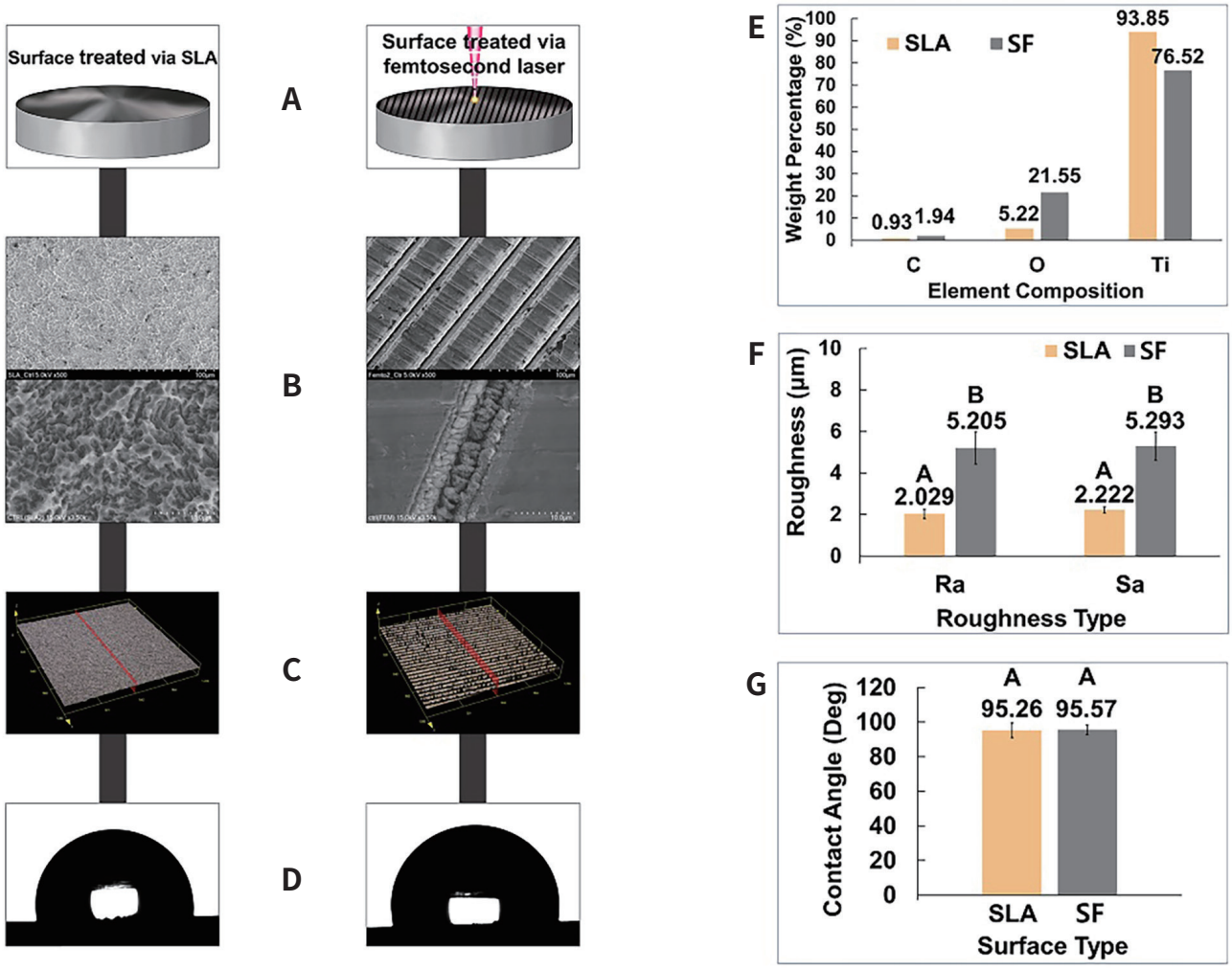

Fig. 2. Surface characteristics of each surface-treated implant disc (left: SLA; right: femtosecond laser). (A) Illustration of implant disc surface treated with SLA and femtosecond laser. (B) Surface observation via scanning electron microscopy. (C) Confocal laser scanning microscopy images according to each surface treatment method. (D) Representative images of contact angle measurements according to each surface treatment method. (E) Element analysis results according to each surface treatment method. (F) Surface roughness measurement results according to each surface treatment method. (G) Contact angle results according to each surface treatment method. Significant differences in Figure 2F and 2G were calculated based on *independent t-test ($P < .05$). The data are presented as mean ± standard deviation (n = 5). Identical letters indicate that difference between the groups is not significant ($P \geq .05$).

confocal laser scanning microscopy (LEXT OLS4100; Olympus, Tokyo, Japan), measuring arithmetic mean roughness (Ra) and arithmetical mean height (Sa) at 10× magnification. Ra was assessed over a length of 1280 μm, and Sa over an area of 456 × 456 μm (Fig. 2C). Wettability evaluation was conducted using a contact angle meter (Phoenix-MT; SEO, Suwon, Korea). A 2-μL droplet of distilled water was formed on each sample surface using a micro syringe. The contact angle between the liquid and sample surfaces was measured from both left and right sides. The contact angle was measured five times per sample, and the average contact angle was calculated (Fig. 2D).

The implant used in this study (s-Clean OneQ-SL; Dentis, Daegu, Korea) was of an internal type with a diameter of 3.9 mm and length of 7 mm. Owing to proprietary issues, detailed manufacturing techniques were not disclosed by the manufacturer. A to-

tal of 20 implant surfaces treated with SLA alone were designated as the SLA group. The 20 implant surfaces treated with femtosecond laser were created by treating the entire area of used SLA implants with the femtosecond laser, designated as the SF group. For surface treatment with a femtosecond laser, the fixture was fixed in a rotating jig and rotated at 50 rpm for 360 degrees. Then, the entire fixation area was irradiated five times with a femtosecond laser, forming a line pattern with 50-μm intervals on the root area (Fig. 1A). The femtosecond laser had a 343-nm wavelength, a scan speed of 0.01 m/s, and a repetition frequency of 200 kHz. The implants were then sterilized after standard cleaning and packaging procedures.

The Institutional Animal Care and Use Committee of the Laboratory Animal Center of Daegu Gyeongbuk Medical Innovation Foundation reviewed and approved the research protocol (approval number: KMEDI-22090202-00). The research methods of the current study and manuscript presentation are compliant with the ARRIVE guidelines. In this study, 10 male New Zealand white rabbits, each weighing approximately 3 kg, were used. After an acclimation period of over 7 days following their arrival, the animals were observed for general symptoms and confirmed to be healthy before experimentation. During the experiment, food and water were provided ad libitum.

For anesthesia, intramuscular injections of ketamine (35 mg/kg)(Ketalar; Yuhan, Seoul, Korea) and xylazine (5 mg/mL)(Rompun; Bayer Korea, Seoul, Korea) were administered, followed by inhalation anesthesia using 1.0% – 2.0% isoflurane (Hana Pharm Co. Ltd., Seoul, Korea) during surgery. The proximal tibia area was shaved and then cleaned with iodine surgical soap. The skin and fascia at the implantation site were incised. Following the manufacturer's instructions, implant placement was performed using a stepwise sequence of spiral drills with saline cooling. A total of 40 implants were placed (N = 40), with four implants placed in each of the 10 rabbits (n = 10), two in each tibia. One implant from the SLA group and one from the SF group were alternately placed in each tibia, resulting in 20 implants per group (N = 20 per group). The implants were positioned alternately in the upper and lower vertical locations of the tibia to minimize variations due to differences in bone thickness (Fig. 1B). Immediately after placement, the ISQ was measured for each implant, and OCT imaging was performed prior to securing the cover screw. The specimen was disinfected using povidone, and a collar was placed around the neck until the sutured area is fully healed. After 4 and 6 weeks of healing, 5 rabbits were anesthetized and sacrificed at each time point with an overdose of intravenous potassium chloride solution. The ISQ values of each implant (Osstell® Beacon device; W&H, Göteborg, Sweden) were measured immediately after placement and post sacrifice (weeks 4 and 6) for comparison.

A commercial SS-OCT system (OCS1310V1, Thorlabs, Inc., Newton, NJ, USA) was used for optical imaging in this study. The system comprises a swept-source light source with a central wavelength of 1310 nm and full width at half maximum bandwidth of > 97 nm (-10 dB cutoff point). The axial scan rate and average laser output were 100 kHz and > 20 mW, respectively. The imaging conditions were set to 7.0 mm × 7.0 mm × 5.0 mm (lateral × vertical × depth), and the image pixel resolution was about 6 μm. These imaging conditions enabled us to reliably acquire images on a system computer equipped with 16 GB of RAM. The acquisition and post-processing of a single set of volume data took around 20 seconds. Optical coherence tomography (OCT) imaging of the top of the implant was performed immediately, week 4, and week 6 post sacrifice to acquire 2D cross-sectional images (Fig. 3). The acquired images were overlaid (immediately and week 4, immediately and week 6) (Fig. 3D), and the area values were measured using the measure function of the image processing software. The marginal bone volume was evaluated within an area of 500 × 500 μm starting from the inner starting point of the top of the implant (Fig. 3E).

Immediately thereafter, implants surgically separated from adjacent bone were fixed in 10% formalin. The fixed samples were washed and soaked in Villanueva bone stain solution for 7 days. After dehydration, the tissue samples were immersed in methyl methacrylate monomer and then embedded in the methyl methacrylate embedding medium resin. The samples were ground and prepared as 40 – 60-μm thick specimens. An optical microscope (IMS 1080P; Sometech Inc., Seoul, Korea) was used to analyze the

https://doi.org/10.4047/jap.2025.17.2.101

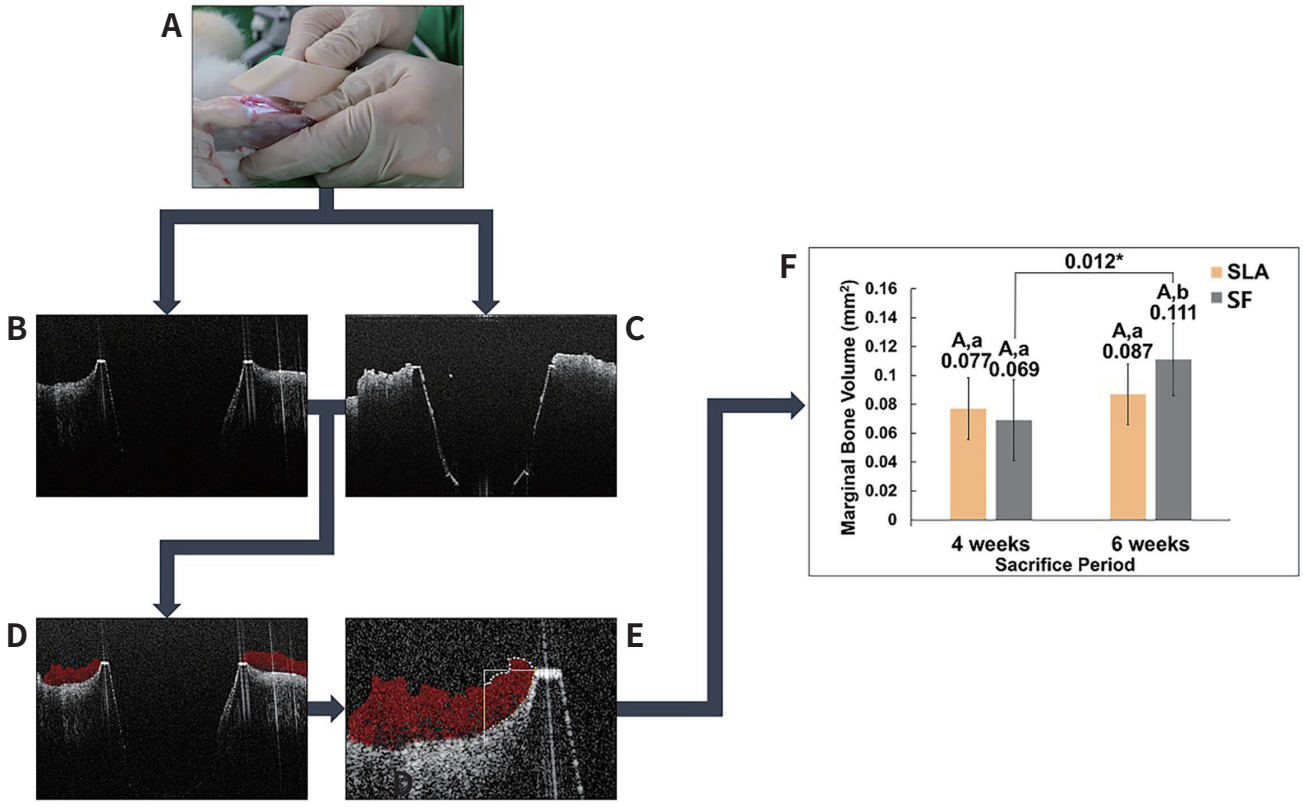

Fig. 3. Process and results for marginal bone volume measurement. (A) Implant placement region imaging via optical coherence tomography. (B) Representative image of implant placement region at 0 weeks. (C) Representative image of implant placement region after recovery. (D) Superimposed results of 0 weeks and post-recovery images (red region indicates increased marginal bone). (E) Measurement process of marginal bone volume. (F) Marginal bone volume measurement results according to each surface treatment method. Significant difference was calculated based on *Wilcoxon signed-rank test ($P < .05$). The data are presented as mean ± standard deviation (n = 20 per group). Identical letters indicate that difference between the groups is not significant ($P \geq .05$).

prepared specimens to acquire images for analysis. The images were used to measure the BV/TV ratio and BIC ratio. Bone volume/tissue volume and BIC measurements were performed as demonstrated in Figure 4. The area from the 3rd to 5th thread on both sides of the implants was used for analysis. The relevant area was photographed at 160× magnification, setting the ROI from the 3rd to 5th thread vertically and a 300-μm area from the apex of the thread horizontally (Fig. 4C). Using an image processing software (NIH ImageJ; NIH., Bethesda, MD, USA), all measurements were performed. BIC measurement involved manual assessment of the direct bone-implant interface by an examiner (Fig. 4D). The implant area of the image was removed, and the stained and unstained areas were differentiated using the threshold function for the BV/TV measurements (Fig. 4F). Only the bone area excluding the implant area was set as the ROI, and the proportion of the white area in the volume of the set area was measured to assess the BV/TV (Fig. 4G).

The statistical software (SPSS release 25.0; IBM Corp., Armonk, NY, USA) was used to analyze all data ($\alpha = 0.05$). Independent t-tests were used to analyze surface roughness and wettability. The Mann-Whitney U test was used to compare marginal bone volume between the SLA and SF groups. The Wilcoxon signed-rank test was used to compare marginal bone volume between weeks 4 and 6 for each surface-treated implant. One-way analysis of variance and independent t-tests were used to compare ISQ measurement re-

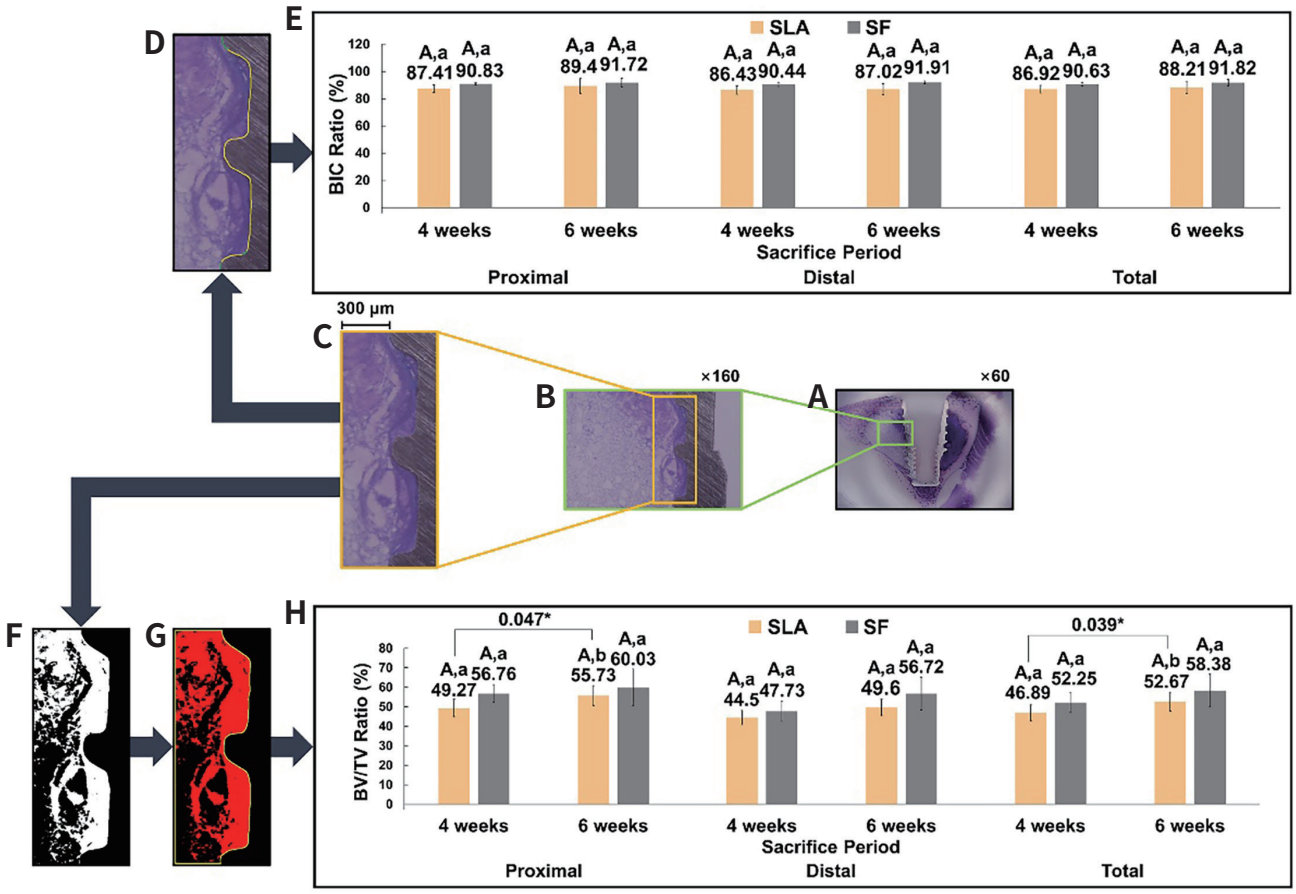

Fig. 4. Bone-to-implant contact (BIC) and bone volume/tissue volume (BV/TV) evaluation process and results via histological analysis. (A) Representative image of histological analysis results (60× magnification). (B) 160× magnified image of the measurement region. (C) Images for BIC and BV/TV evaluation (evaluation area: the 3rd to 5th thread of implant, 300-μm range on either side of apex of the 3rd thread). (D) BIC ratio measurement process (the yellow line represents bone, the green line represents no contact; the total length of both lines was used to calculate the ratio of the yellow line, indicating the percentage of BIC). (E) BIC measurement results according to each surface treatment method. (F) Filtered image for BV/TV measurements. (G) Measurement range of BV/TV (in the yellow area, the red area represents bone). (H) BV/TV ratio measurement results according to each surface treatment method.
*Significant difference was calculated based on Wilcoxon signed-rank test ($P < .05$). The data are presented as mean ± standard deviation (n = 20 per group). Identical letters indicate that difference between the groups is not significant ($P \geq .05$).

Table 1. Comparison of ISQ values after placement of each surface-treated implant

Group	Implant stability quotient			F	*P***
	0 weeks	4 weeks	6 weeks		
SLA	59.7 ± 11.7^{A}	77.2 ± 3.2^{B}	78.8 ± 5.2^{B}	7.651	.011**
SF	59.5 ± 10.9^{A}	75.5 ± 5.4^{B}	79.2 ± 3.4^{B}	8.275	.009**
T	0.31	0.539	-0.147		
*P**	.976	.609	.888		

ISQ, implant stability quotient; SLA, sandblasting large grit acid-etching; SF, implant surface treated with a femtosecond laser on the SLA surface.
Significant difference was calculated based on *independent t-test and **one-way analysis of variance ($P < .05$).
Same superscript uppercase letters are not significantly different according to the Scheffé's test ($P \geq .05$).

https://doi.org/10.4047/jap.2025.17.2.101

sults over time for each surface-treated implant and between treatment methods. Mann-Whitney U tests and Wilcoxon signed-rank tests were used to compare BIC and BV/TV results between treatment methods and over time for each implant.

RESULTS

The surface treated with SLA was characterized by microgrooves due to sandblasting and acid-etching, demonstrating a finely rough surface with evenly distributed porosity. The surface treated with a femtosecond laser showed a consistent linear pattern with spherical microstructures within the altered patterns, indicating an increase in roughness. Figure 2E and Supplemental Table 1 summarize the results of element analysis for surfaces treated with SLA and a femtosecond laser. Comparing both surfaces, the carbon content showed no significant difference; however, the oxygen content was higher and the titanium content was lower in the surface treated with a femtosecond laser. Figure 2C and Supplemental Table 2 illustrate the differences in the surface roughness (Ra and Sa) based on the treatment method, showing profiles of surfaces treated with SLA on the left and those of surfaces treated with a femtosecond laser on the right. The surface treated with a femtosecond laser showed significantly higher roughness in both Ra and Sa than the surface treated with SLA (Ra: SLA = 2.09 ± 0.451, Femtosecond laser = 5.205 ± 1.571; Sa: SLA = 2.222 ± 0.305, Femtosecond laser = 5.293 ± 1.349; $P < .05$). Figure 2D and Supplemental Table 3 depict the wettability based on the surface treatment method. The droplets formed on the surfaces treated with SLA and a femtosecond laser demonstrated similar shapes. The surface contact angles were comparable, with no significant differences (SLA = 95.26 ± 8.70, Femtosecond laser = 95.57 ± 5.70; $P > .05$).

As shown in Table 1, the immediate and post implantation (4 weeks and 6 weeks) ISQ values of the SLA and SF (surface treated with femtosecond laser) groups were compared. No significant differences were observed between the SLA and SF groups at 0, 4, and 6 weeks (0 weeks: SLA = 59.7 ± 11.7, SF = 59.5 ± 10.9; 4 weeks: SLA = 77.2 ± 3.2, SF = 75.5 ± 5.4; 6 weeks: SLA = 78.8 ± 5.2, SF = 79.2 ± 3.4; $P > .05$). However, within each group, a significant increase in ISQ values was observed over the recovery periods (0, 4, and 6 weeks) ($P < .05$).

As shown in Figure 3F and Supplemental Table 4, the marginal bone volumes of the SLA and SF groups were compared. No significant differences were noted between the two groups at weeks 4 and 6 (4 weeks: SLA = 0.077 ± 0.043, SF = 0.069 ± 0.048; 6 weeks: SLA = 0.087 ± 0.042, SF = 0.111 ± 0.050; $P > .05$). Although the SLA implants demonstrated no significant difference between weeks 4 and 6 ($P > .05$), the SF group showed a significant difference in marginal bone volume between these two time points ($P < .05$).

The BIC (Figure 4E and Supplemental Table 5) and BV/TV (Figure 4H and Supplemental Table 6) were compared between the SLA and SF groups. Regarding BIC, no significant differences were observed between the proximal, distal, and total groups (Proximal, 4 weeks: SLA = 49.27 ± 9.05, SF = 56.76 ± 9.26; 6 weeks: SLA = 55.73 ± 10.28, SF = 60.03 ± 18.68; Distal, 4 weeks: SLA = 44.50 ± 7.45, SF = 47.73 ± 10.40; 6 weeks: SLA = 49.60 ± 8.53, SF = 56.72 ± 16.93; Total, 4 weeks: SLA = 46.89 ± 8.29, SF = 52.25 ± 10.51; 6 weeks: SLA = 52.67 ± 9.56, SF = 58.38 ± 17.09; $P > .05$). Similarly, no significant differences were noted in BIC between weeks 4 and 6 within each group. In the BV/TV comparison, no significant differences were observed among the proximal, distal, and total groups ($P > .05$). However, a significant difference in BV/TV was noted in the SLA group between weeks 4 and 6 in the proximal and total groups ($P < .05$).

DISCUSSION

This study used SEM to observe surface characteristics, revealing distinct surface patterns between SLA and femtosecond laser-treated surfaces. Element composition differences were confirmed via EDS. Surface roughness, measured in Ra and Sa, was higher in the femtosecond laser-treated surfaces, although wettability was similar for both treatments. For both surface types, ISQ comparison after implantation demonstrated similar values. However, a significant increase in ISQ over the recovery period was observed for both surfaces, suggesting adequate bone-implant integration after 4 weeks. Mar-

ginal bone volume comparison between the SLA and SF groups demonstrated similarity; however, a more significant growth in marginal bone at 6 weeks was observed in the SF group, indicating a positive role in marginal bone growth for both SLA and femtosecond laser-treated implants. Histological analysis comparing BIC and BV/TV for both surfaces revealed similar results in all measurement areas. Thus, although surface treatment influenced surface morphology, composition, and roughness, it did not show a significant difference in bone integration assessments, partially rejecting the second null hypothesis.

Micro- and nanostructures on implant surfaces enhance bone fixation.[1-7,35] Thor *et al*.[36] reported that porous titanium implants with microstructures enhanced early-stage bone integration. Park *et al*.[37] also reported a significant influence of surface chemical composition and microstructure on blood response and bone integration. This study confirmed the surface characteristics and composition via SEM and EDS, respectively. Femtosecond laser treatment created linear patterns and spherical microstructures on the surface, increasing the roughness. Gnilitskyi *et al*.[38] reported that linear structures created by femtosecond lasers enhanced cell growth rates. The present study found comparable or superior results for ISQ, marginal bone volume, BV/TV, and BIC with femtosecond laser-treated surfaces compared with widely used SLA treatments. Previous studies have shown low roughness in SLA surfaces, affecting bacterial adhesion.[14,15] The present study noted higher roughness with femtosecond laser treatment than with SLA using confocal laser scanning microscopy images, with average Ra and Sa values of 5.205 and 5.293, respectively. No implant failures or peri-implantitis were observed during the study period despite higher roughness, underscoring the effect of femtosecond laser surface roughness on bone integration. However, with the short observation period for bone integration and the inability to evaluate bacterial presence, further research is warranted.

A previous study has shown positive effects of SLA-treated surfaces on implant stabilization post-implantation,[39] and femtosecond laser-treated surfaces have remarkably enhanced the adhesion of endothelial cells and bone marrow mesenchymal stem cells. However, no studies have combined SLA and femtosecond laser treatments. This study aimed to combine both treatments to observe their synergistic benefits. Based on a previous study, a femtosecond laser was applied to the root area, which was larger than the thread area, to reduce bacterial infection and enhance bone integration.[19,24,25] The femtosecond laser was applied over 50-μm spaced lines, complementing untreated areas with the prevalent SLA surface treatment (Fig. 1A).

ISQ, ranging from 1 to 100, with the values of 57 to 82 suggesting sufficient stability,[40] is a commonly used method to evaluate implant fixation. In a previous study, ISQ was measured on various implant surfaces to confirm stability.[41] This study showed no significant difference in ISQ values between the SLA and SF groups immediately after implantation and at weeks 4 and 6, indicating that both SLA treatment and combined SLA and femtosecond laser surface treatments achieved excellent bone integration. Ernst *et al*.[42] compared traditional SLA implants with implants having a highly crystalline and phosphate-enriched anodized titanium oxide surface, revealing similar ISQ results and suggesting the viability of new surface treatments. Similarly, the present study revealed comparable results for the SLA and SF groups, indicating the feasibility of SLA and femtosecond laser surface treatments within the limitations of the present study.

The marginal bone plays a critical role in implant fixation post-implantation. Marginal bone loss, caused by peri-implantitis, and excessive occlusal forces can threaten implant lifespan, with bacteria being the primary cause. Seo *et al*.[15] reported that femtosecond laser surface treatment suppressed the action of Porphyromonasgingivalis and Prevotella intermedia on titanium discs. Other studies have also reported the bacteriostatic effect of femtosecond laser-treated surfaces on Pg bacteria present on zirconia discs.[24] Thus, femtosecond laser surface treatment may have inhibited bacterial formation, reducing marginal bone loss and increasing bone volume. To the best of our knowledge, no studies have used OCT to evaluate marginal bone volume. The present study acquired data on marginal bone above implants immediately after the procedure and at 4- and

https://doi.org/10.4047/jap.2025.17.2.101

6-weeks using OCT and revealed no significant difference between the SLA and SF groups. This shows the appropriateness of OCT for comparing marginal bone growth. Although difficult to compare with other studies, previous research has also assessed marginal bone after various surface treatments, evaluating the influence of the surface.[43] In the present study, no difference was found in the surface treatment methods; however, the SF group demonstrated increased marginal bone volume over time compared with the SLA group, indicating the benefits of SLA and femtosecond laser surface treatments for marginal bone growth.

Tissue morphological analysis was performed for evaluating bone integration. Previous studies have extensively conducted histological analysis to confirm bone integration post-implantation. Wedemeyer *et al*.[5] compared titanium implants with nanoscale structures induced by laser with traditional implants through histological analysis of BIC and BV/TV, indicating the clinical suitability of laser techniques for creating nanostructures. This study revealed no significant difference in BIC and BV/TV between the SLA and SF groups. However, the SLA group revealed a significant increase in BV/TV over time (4 and 6 weeks). Previous research has indicated that titanium implants with nanoscale surface characteristics enhance early-stage bone integration.[44] Although no significant differences were noted in the present study, all BV/TV ratios were higher in the SF group than in the SLA group, suggesting superior early-stage bone integration in the SF group. Thus, within the limits of the present study, implants with surfaces treated with SLA and femtosecond lasers can be compared with those treated with SLA alone. However, as no statistically significant differences were noted in BIC and BV/TV compared with SLA, further research is warranted to explore effective patterning methods. Additional studies on femtosecond laser-treated implants *in vivo* and bacterial formation are anticipated.

This study compared implants treated with SLA and those treated with combined SLA and a femtosecond laser. However, implants treated solely with femtosecond lasers were not evaluated. Additionally, various laser surface patterns were not explored, and only the root area of implants was subjected to laser surface treatment. Biofilm observation of implants and prolonged observation for implant success were not conducted. Thus, the present study results should be interpreted with caution, and future research should overcome the limitations of this study.

CONCLUSION

The present study compared implants treated with SLA and those treated with both SLA and femtosecond laser, revealing no impact on ISQ, marginal bone volume, BIC, or BV/TV. Although no significant differences were noted in BIC and BV/TV comparisons, all values were higher for implants treated with both SLA and femtosecond laser. Thus, within the limits of the present study, the combined surface treatment method of SLA and femtosecond laser has proven viable compared with the widely used SLA surface treatment method. However, despite these findings, further stringent research on superior surface patterns and bacterial formation is required for the clinical application of this technology.

ACKNOWLEDGMENTS

The authors thank the researchers at the Advanced Dental Device Development Institute, Kyungpook National University, for their time and contribution to the study.

REFERENCES

1. Bissinger O, Götz C, Jeschke A, Haller B, Wolff KD, Kaiser P, Kolk A. Comparison of contact radiographed and stained histological sections for osseointegration analysis of dental implants: an in vivo study. Oral Surg Oral Med Oral Pathol Oral Radiol 2018;125:20-6.
2. Musskopf ML, Finger Stadler A, Wikesjö UM, Susin C. The minipig intraoral dental implant model: a systematic review and meta-analysis. PLoS One 2022;17:e0264475.
3. Rizo-Gorrita M, Fernandez-Asian I, Garcia-de-Frenza A, Vazquez-Pachon C, Serrera-Figallo MA, Torres-Lagares D Gutierrez-Perez JL. Influence of three dental implant surfaces on cell viability and bone behavior. An in vitro and a histometric study in a rabbit model. Ap-

pl Sci 2020;10:4790.
4. Velasco-Ortega E, Ortiz-Garcia I, Jiménez-Guerra A, Núñez-Márquez E, Moreno-Muñoz J, Rondón-Romero JL, Cabanillas-Balsera D, Gil J, Muñoz-Guzón F, Monsalve-Guil L. Osseointegration of sandblasted and acid-etched implant surfaces. A histological and histomorphometric study in the rabbit. Int J Mol Sci 2021; 22:8507.
5. Wedemeyer C, Jablonski H, Mumdzic-Zverotic A, Fietzek H, Mertens T, Hilken G, Krüger C, Wissmann A, Heep H, Schlepper R, Kauther MD. Laser-induced nanostructures on titanium surfaces ensure osseointegration of implants in rabbit femora. Materialia 2019;6:100266.
6. Kumar PS, KS SK, Grandhi VV, Gupta V. The effects of titanium implant surface topography on osseointegration: literature review. JMIR Biomed Eng 2019;4: e13237.
7. Petrini M, Pierfelice TV, D'Amico E, Di Pietro N, Pandolfi A, D'Arcangelo C, De Angelis F, Mandatori D, Schiavone V, Piattelli A, Iezzi G. Influence of nano, micro, and macro topography of dental implant surfaces on human gingival fibroblasts. Int J Mol Sci 2021;22:9871.
8. Song YW, Paeng KW, Kim MJ, Cha JK, Jung UW, Jung RE, Thoma DS. Secondary stability achieved in dental implants with a calcium-coated sandblasted, large-grit, acid-etched (SLA) surface and a chemically modified SLA surface placed without mechanical engagement: a preclinical study. Clin Oral Implants Res 2021; 32:1474-83.
9. Han A, Li X, Huang B, Tsoi JKH, Matinlinna JP, Chen Z, Deng DM. The effect of titanium implant surface modification on the dynamic process of initial microbial adhesion and biofilm formation. Int J Adhesion Adhes 2016;69:125-32.
10. Siddiqui DA, Guida L, Sridhar S, Valderrama P, Wilson TG Jr, Rodrigues DC. Evaluation of oral microbial corrosion on the surface degradation of dental implant materials. J Periodontol 2019;90:72-81.
11. Liu R, Tang Y, Liu H, Zeng L, Ma Z, Li J, Zhao Y, Ren L, Yang K. Effects of combined chemical design (Cu addition) and topographical modification (SLA) of Ti-Cu/SLA for promoting osteogenic, angiogenic and antibacterial activities. J Mater Sci Technol 2020;47:202-15.
12. Simões IG, Dos Reis AC, da Costa Valente ML. Analysis of the influence of surface treatment by high-power laser irradiation on the surface properties of titanium dental implants: a systematic review. J Prosthet Dent 2023;129:863-70.
13. Abdal-hay A, Staples R, Alhazaa A, Fournier B, Al-Gawati M, Lee RSB, Ivanovski S. Fabrication of micropores on titanium implants using femtosecond laser technology: Perpendicular attachment of connective tissues as a pilot study. Opt Laser Technol 2022;148: 107624.
14. Bihn SK, Son K, Son YT, Dahal RH, Kim S, Kim J, Hwang JH, Kwon SM, Lee JH, Kim HD, Lee JM, Jin MU, Lee KB. In vitro biofilm formation on zirconia implant surfaces treated with femtosecond and nanosecond lasers. J Funct Biomater 2023;14:486.
15. Seo BY, Son K, Son YT, Dahal RH, Kim S, Kim J, Hwang J, Kwon SM, Lee JM, Lee KB, Kim JW. Influence of dental titanium implants with different surface treatments using femtosecond and nanosecond lasers on biofilm formation. J Funct Biomater 2023;14:297.
16. Tzanakakis EC, Skoulas E, Pepelassi E, Koidis P, Tzoutzas IG. The use of lasers in dental materials: a review. Materials (Basel) 2021;14:3370.
17. Sun H, Li J, Liu M, Yang D, Li F. A review of effects of femtosecond laser parameters on metal surface properties. Coatings 2022;12:1596.
18. Lee JS, Son K, Hwang SM, Son YT, Kim YG, Suh JY, Hwang JH, Kwon SM, Lee JH, Kim HD, Lee KB, Lee JM. Effect of electrocautery and laser treatment on the composition and morphology of surface-modified titanium implants. Bioengineering (Basel) 2023;10: 1251.
19. Eun SM, Son K, Hwang SM, Son YT, Kim YG, Suh JY, Hwang JH, Kwon SM, Lee JH, Kim HD, Lee KB, Lee JM. The impact of mechanical debridement techniques on titanium implant surfaces: a comparison of sandblasted, acid-etched, and femtosecond laser-treated surfaces. J Funct Biomater 2023;14:502.
20. Gianfreda F, Antonacci D, Raffone C, Muzzi M, Pistilli V, Bollero P. Microscopic characterization of bioactivate implant surfaces: increasing wettability using salts and dry technology. Materials (Basel) 2021;14:2608.
21. Toffoli A, Parisi L, Tatti R, Lorenzi A, Verucchi R, Manfredi E, Lumetti S, Macaluso GM. Thermal-induced hydrophilicity enhancement of titanium dental implant surfaces. J Oral Sci 2020;62:217-21.

22. Scarano A, Tari Rexhep S, Leo L, Lorusso F. Wettability of implant surfaces: blood vs autologous platelet liquid (APL). J Mech Behav Biomed Mater 2022;126:104773.
23. Yu YJ, Zhu WQ, Xu LN, Ming PP, Shao SY, Qiu J. Osseointegration of titanium dental implant under fluoride exposure in rabbits: Micro-CT and histomorphometry study. Clin Oral Implants Res 2019;30:1038-48.
24. Al Deeb M, Aldosari AA, Anil S. Osseointegration of tantalum trabecular metal in titanium dental implants: histological and micro-CT study. J Funct Biomater 2023;14:355.
25. Scarano A, Orsini T, Di Carlo F, Valbonetti L, Lorusso F. Graphene-doped poly (Methyl-Methacrylate) (Pmma) implants: a micro-CT and histomorphometrical study in rabbits. Int J Mol Sci 2021;22:1441.
26. Gehrke SA, Prados-Frutos JC, Prados-Privado M, Calvo-Guirado JL, Aramburú Júnior J, Pérez-Díaz L, Mazón P, Aragoneses JM, De Aza PN. Biomechanical and histological analysis of titanium (machined and treated surface) versus zirconia implant materials: an in vivo animal study. Materials (Basel) 2019;12:856.
27. Jinno Y, Stocchero M, Galli S, Toia M, Becktor JP. Impact of a Hydrophilic Dental Implant Surface on Osseointegration: Biomechanical Results in Rabbit. J Oral Implantol 2021;47:163-8.
28. Hériveaux Y, Vayron R, Fraulob M, Lomami HA, Lenormand C, Haïat G. Assessment of dental implant stability using resonance frequency analysis and quantitative ultrasound methods. J Prosthodont Res 2021;65:421-7.
29. Kang SJ, Park JB, Kim I, Lee W, Kim H. Evaluation of apically positioned dental implants with a sandblasted with large grit and acid-etched surface 1 day after initial placement using micro-CT images and non-decalcified tissue slide images in a rabbit model. Int J Oral Maxillofac Implants 2019;34:1078-83.
30. López-Valverde N, López-Valverde A, Cortés MP, Rodríguez C, Macedo De Sousa B, Aragoneses JM. Bone quantification around chitosan-coated titanium dental implants: a preliminary study by micro-CT analysis in jaw of a canine model. Front Bioeng Biotechnol 2022;10:858786.
31. Padala SR, Asikainen P, Ruotsalainen T, Mikkonen JJ, Silvast TS, Koistinen AP, Schulten EAJM, Ten Bruggenkate CM, Kullaa AM. Effects of irradiation in the mandibular bone loaded with dental implants. An experimental study with a canine model. Ultrastruct Pathol 2021;45:276-85.
32. Son K, Cho H, Kim H, Lee W, Cho M, Jeong H, Kim KH, Lee DH, Kim SY, Lee KB, Jeon M, Kim J. Dental diagnosis for inlay restoration using an intraoral optical coherence tomography system: a case report. J Prosthodont Res 2023;67:305-10.
33. Son K, Koo B, Lee W, Cho M, Lee HC, Kim KH, Jeong H, Jeon M, Kim J, Lee KB. A concept to detect a subgingival finish line using an intraoral optical coherence tomography system: a clinical report. J Prosthet Dent 2023:S0022-3913(23)00696-0. Epub ahead of print.
34. Kim Y, Jung GI, Jeon D, Wijesinghe RE, Seong D, Lee J, Do WJ, Kwon SM, Lee JH, Hwang JH, Kim HD, Lee KB, Jeon M, Kim J. Non-invasive optical coherence tomography data-based quantitative algorithm for the assessment of residual adhesive on bracket-removed dental surface. Sensors (Basel) 2021;21:4670.
35. Yeo IL. Modifications of dental implant surfaces at the micro- and nano-level for enhanced osseointegration. Materials (Basel) 2019;13:89.
36. Thor A, Rasmusson L, Wennerberg A, Thomsen P, Hirsch JM, Nilsson B, Hong J. The role of whole blood in thrombin generation in contact with various titanium surfaces. Biomaterials 2007;28:966-74.
37. Park JY, Gemmell CH, Davies JE. Platelet interactions with titanium: modulation of platelet activity by surface topography. Biomaterials 2001;22:2671-82.
38. Gnilitskyi I, Pogorielov M, Viter R, Ferraria AM, Carapeto AP, Oleshko O, Orazi L, Mishchenko O. Cell and tissue response to nanotextured Ti6Al4V and Zr implants using high-speed femtosecond laser-induced periodic surface structures. Nanomedicine 2019;21:102036.
39. Zarazir R, Mrad S, Aoun G, Sleiman AA, Mousallem M, Bassil J. Comparison of osseointegration in novel laser-textured and SLA implants. Acta Inform Med 2023;31:137-40.
40. Balleri P, Cozzolino A, Ghelli L, Momicchioli G, Varriale A. Stability measurements of osseointegrated implants using Osstell in partially edentulous jaws after 1 year of loading: a pilot study. Clin Implant Dent Relat Res 2002;4:128-32.
41. Carmo Filho LCD, Marcello-Machado RM, Castilhos ED, Del Bel Cury AA, Faot F. Can implant surfaces af-

fect implant stability during osseointegration? A randomized clinical trial. Braz Oral Res 2018;32:e110.
42. Ernst S, Stübinger S, Schüpbach P, Sidler M, Klein K, Ferguson SJ, von Rechenberg B. Comparison of two dental implant surface modifications on implants with same macrodesign: an experimental study in the pelvic sheep model. Clin Oral Implants Res 2015;26:898-908.
43. Abrahamsson I, Berglundh T. Effects of different implant surfaces and designs on marginal bone-level alterations: a review. Clin Oral Implants Res 2009;20 Suppl 4:207-15.
44. Souza JCM, Sordi MB, Kanazawa M, Ravindran S, Henriques B, Silva FS, Aparicio C, Cooper LF. Nano-scale modification of titanium implant surfaces to enhance osseointegration. Acta Biomater 2019;94:112-31.

Supplemental Table 1. Weight percentage of elements according to each surface-treated implant disc

Group	Weight percentage (%)			
	C	O	Ti	Al
SLA	1.31	5.6	93.09	-
	0.55	4.83	94.61	-
Femtosecond laser	2.24	23.77	73.99	-
	1.64	19.32	79.05	-

C, carbon; O, oxygen; Ti, titanium; Al, aluminum; SLA, sandblasting large grit acid-etching.

Supplemental Table 3. Comparison of surface contact angles according to each implant disc surface treatment method

Surface type	Mean ± SD (°)	T	*P**
SLA	95.26 ± 8.70	0.104	.918
Femtosecond laser	95.57 ± 5.70		

SD, standard deviation; SLA, sandblasted, large grit, and acid-etched.
Significant difference determined by *independent t-test ($P < .05$).

Supplemental Table 2. Comparison of surface roughness according to each surface-treated implant disc

Roughness type	Surface type	Mean ± SD (μm)	T	*P**
Ra	SLA	2.029 ± 0.451	-4.345	.002*
	Femtosecond laser	5.205 ± 1.571		
Sa	SLA	2.222 ± 0.305	-4.966	.006*
	Femtosecond laser	5.293 ± 1.349		

SD, standard deviation; Ra, average surface roughness; Sa, average absolute surface roughness; SLA, sandblasting large grit acid-etching.
Significant difference was calculated based on *independent t-test ($P < .05$).

Supplemental Table 4. Comparison of marginal bone volume according to each surface-treated implant

Group	Marginal bone volume (mm^2) Mean ± SD		Z	*P***
	4 weeks	6 weeks		
SLA	0.077 ± 0.043	0.087 ± 0.042	-0.259	.41
SF	0.069 ± 0.048	0.111 ± 0.050	-2.223	.012**
Z	0.641	1.394		
*P**	0.266	0.086		

SD, standard deviation; SLA, sandblasting large grit acid-etching; SF, implant surface treated with a femtosecond laser on the SLA surface.
Significant difference was calculated based on *Mann-Whitney U test and **Wilcoxon signed-rank test ($P < .05$).

https://doi.org/10.4047/jap.2025.17.2.101

Supplemental Table 5. BIC ratio comparison via histological analysis according to each implant surface treatment method

Site	Sacrifice period	BIC ratio (%) Mean ± SD		*P**	SLA; *P***	SF; *P****
		SLA	SF			
Proximal	4 weeks	87.41 ± 5.49	90.83 ± 1.63	.12	.281	.422
	6 weeks	89.40 ± 11	91.72 ± 6.54	.469		
Distal	4 weeks	86.43 ± 6.11	90.44 ± 3.09	.197	.5	.109
	6 weeks	87.02 ± 7.92	91.91 ± 2.12	.09		
Total	4 weeks	86.92 ± 5.56	90.63 ± 2.37	.08	.339	.133
	6 weeks	88.21 ± 9.22	91.82 ± 4.64	.159		

BIC, bone-to-implant contact; SD, standard deviation; SLA, sandblasting large grit acid-etching; SF, implant surface treated with a femtosecond laser on the SLA surface.
*Significant difference was calculated based on Mann-Whitney U test ($P < .05$). ** and *** Wilcoxon signed-rank test ($P < .05$).

Supplemental Table 6. BV/TV ratio comparison via histological analysis according to each implant surface treatment method

Site	Sacrifice period	BV/TV ratio (%) Mean ± SD		*P**	SLA; *P***	SF; *P****
		SLA	SF			
Proximal	4 weeks	49.27 ± 9.05	56.76 ± 9.26	.155	.047**	.422
	6 weeks	55.73 ± 10.28	60.03 ± 18.68	.409		
Distal	4 weeks	44.50 ± 7.45	47.73 ± 10.40	.35	.156	.281
	6 weeks	49.60 ± 8.53	56.72 ± 16.93	.35		
Total	4 weeks	46.89 ± 8.29	52.25 ± 10.51	.133	.039**	.235
	6 weeks	52.67 ± 9.56	58.38 ± 17.09	.489		

BV/TV, bone volume/tissue volume; SD, standard deviation; SLA, sandblasting large grit acid-etching; SF, implant surface treated with a femtosecond laser on the SLA surface.
*Significant difference was calculated using Mann-Whitney U test ($P < .05$). ** and *** Wilcoxon signed-rank test ($P < .05$).